Maximal Zero Textures in Linear and Inverse Seesaw

Roopam Sinha[*], **Rome Samanta**[†], **Ambar Ghosal**[‡]
Saha Institute of Nuclear Physics, 1/AF Bidhannagar, Kolkata 700064, India

June 7, 2016

Abstract

We investigate Linear and Inverse seesaw mechanisms with maximal zero textures of the constituent matrices subjected to the assumption of non-zero eigenvalues for the neutrino mass matrix m_ν and charged lepton mass matrix m_e. If we restrict to the minimally parametrized non-singular 'm_e' (i.e., with maximum number of zeros) it gives rise to only 6 possible textures of m_e. Non-zero determinant of m_ν dictates six possible textures of the constituent matrices. We ask in this minimalistic approach, what are the phenomenologically allowed maximum zero textures are possible. It turns out that Inverse seesaw leads to 7 allowed two-zero textures while the Linear seesaw leads to only one. In Inverse seesaw, we show that 2 is the maximum number of independent zeros that can be inserted into μ_S to obtain all 7 viable two-zero textures of m_ν. On the other hand, in Linear seesaw mechanism, the minimal scheme allows maximum 5 zeros to be accommodated in 'm' so as to obtain viable effective neutrino mass matrices (m_ν). Interestingly, we find that our minimalistic approach in Inverse seesaw leads to a realization of all the phenomenologically allowed two-zero textures whereas in Linear seesaw only one such texture is viable. Next our numerical analysis shows that none of the two-zero textures give rise to enough CP violation or significant δ_{CP}. Therefore, if $\delta_{CP} = \pi/2$ is established, our minimalistic scheme may still be viable provided we allow more number of parameters in 'm_e'.

[*]roopam.sinha@saha.ac.in
[†]rome.samanta@saha.ac.in
[‡]ambar.ghosal@saha.ac.in

1 Introduction

In Type-I seesaw mechanism the lightness of the observed neutrinos are attributed to a seesaw scale around the GUT scale incorporated in the theory. In this mechanism, right-handed neutrinos (ν_R) incorporated in the seesaw scale are usually identified with the mass of the ν_R: (M_{ν_R}) lightest of which is constrained from leptogenesis as $M_{\rm lightest} \geq 10^8$ GeV [1, 2]. Probing the new physics at such a high scale is far beyond the reach of ongoing collider experiments. Moreover, apart from experimental accessibility, a theoretical analysis based on naturalness for a hierarchical ν_R masses ($M_{R_3} > M_{R_2} > M_{R_1}$) put constraints on them as [3]:

$$M_{R_1} \leq 4 \times 10^7 \text{GeV}, \;\; M_{R_2} \leq 7 \times 10^7 \text{GeV}, \;\; M_{R_3} \leq 3 \times 10^7 \text{GeV} (\frac{0.05eV}{m_{min}})^{\frac{1}{3}} \tag{1.1}$$

where m_{min} is the mass of the lightest neutrino. On the other hand, a seesaw scale in the TeV range can be realized in some other variants, such as Inverse seesaw, Linear seesaw etc. by paying the price in terms of addition of extra singlet neutral fermions into these mechanisms which can explain the smallness of neutrino mass by a small lepton-number breaking mass matrix. The ingredients of these two models incorporate, in addition to the Standard Model singlet right-handed neutrinos $\{\nu_{\alpha R}\}$, a set of singlet fermions $\{S_{\beta R}\}$, where α, β (=1,2,3) are the flavour indices. The Yukawa sector of such low energy seesaw mechanism is described by the Lagrangian [4–16]

$$\begin{aligned} -\mathcal{L}_{mass} = \overline{\nu_{\alpha L}} m_D^{\alpha\beta} \nu_{\beta R} + M_R^{\alpha\beta} \overline{(\nu_{\alpha R})^c} \nu_{\beta R} + M_L^{\alpha\beta} \overline{\nu_{\alpha L}} (\nu_{\beta L})^c + \mu_S^{\alpha\beta} \overline{(S_{\alpha R})^c} S_{\beta R} \\ + \overline{\nu_{\alpha L}} M^{\alpha\beta} S_{\beta R} + m^{\alpha\beta} \overline{(\nu_{\alpha R})^c} S_{\beta R} + h.c. \end{aligned} \tag{1.2}$$

$$= \begin{pmatrix} \overline{\nu_{\alpha L}} & \overline{(\nu_{\beta R})^c} & \overline{(S_{\beta R})^c} \end{pmatrix} \begin{pmatrix} M_L & m_D & M \\ m_D^T & M_R & m \\ M^T & m & \mu_S \end{pmatrix} \begin{pmatrix} (\nu_{\beta L})^c \\ \nu_{\beta R} \\ S_{\beta R} \end{pmatrix} + h.c. \tag{1.3}$$

where m_D, M, m (since it is due to combination of two different fields) are the Dirac type and the rest are the Majorana type mass matrices. Usually the Linear seesaw mechanism is facilitated with the exclusion of all other lepton number violating mass terms expect 'm' whereas in Inverse seesaw mechanism both μ_S and m contain lepton number violating mass terms. Thus for Linear seesaw, we consider diagonal entries $M_L = M_R = \mu_S = 0$ and for Inverse seesaw, $M_L = M_R = M = 0$. Therefore, the low energy effective neutrino mass matrix in Linear seesaw [17–21] can be written as

$$m_\nu \;\; \approx \;\; -M(m^{-1} m_D^T) - [M(m^{-1} m_D^T)]^T \tag{1.4}$$

and accordingly in Inverse seesaw it turns out as

$$m_\nu \;\; \approx \;\; m_D m^{-1} \mu_S (m_D m^{-1})^T. \tag{1.5}$$

Now as there are fewer number of experimental constraints, a fruitful approach is to minimize the number of parameters in the Lagrangian. Popular paradigm is to consider some symmetry in the Lagrangian that reduces the number of parameters or to assume texture zeros (which are also dictated by some underlying symmetry) in the fundamental mass matrices.

In our present work we investigate both the low energy seesaw mechanisms mentioned earlier, incorporating the idea of maximal zero textures [22–41] subjected to the criterion of non-zero eigenvalues of the charged lepton (m_e) and effective neutrino mass matrix (m_ν). We investigate the viable textures of m_ν with maximum number of zeros that can be accommodated with the current data. Our methodology is as follows:
i) First we explore to find out a minimal texture of charged lepton mass matrix (m_e) which gives rise to three distinct nonzero eigenvalues, i.e, minimum number of parameters necessary to obtain $\det(m_e m_e^\dagger) \neq 0$. The textures obtained are such that they do not contribute to U_{PMNS}.
ii) Next we assume all the three light neutrino eigenvalues of m_ν are non-zero i.e., $\det(m_\nu) \neq 0$. The Linear seesaw formula implies that m_D, m and M are also non-singular. This fact unambiguously determines the possible minimal textures of m_D, m and M. In the Inverse seesaw, the same criterion fixes the minimal textures of m_D, μ_S and m.
iii) Fixing a particular minimal structure of m_D and M in Linear seesaw (or m_D and m in Inverse Seesaw), we systematically explore to obtain the minimal texture of the matrix m (in Linear Seesaw) and μ_S in Inverse Seesaw by putting zeros in different entries, for the case of Linear (Inverse) seesaw.
iv) Following, we utilize the Frampton and Glashow and Marfatia condition [22] to eliminate emerged unphysical effective neutrino matrices (m_ν).
v) Finally, we explore numerically the parameter space of the survived matrices utilizing the neutrino oscillation global fit data and predict $\Sigma_i m_i$, $|m_{11}|$, J_{CP}, δ_{CP} along with the hierarchical structure of neutrino masses.
The paper is organized as follows: Sec. 2 contains minimally parametrized charged lepton mass matrices m_e and it is obtained that they do not contribute to U_{PMNS}. Effective neutrino mass matrices arising from texture zeros in Linear seesaw is discussed in Sec. 3. The same analysis for Inverse seesaw in presented in Sec. 4. Sec. 5 contains the summary of the present work.

2 The minimal charged lepton basis

In general, the charged lepton mass matrix has the form

$$m_e = \begin{pmatrix} A'e^{ia'} & B'e^{ib'} & C'e^{ic'} \\ D'e^{id'} & E'e^{ie'} & F'e^{if'} \\ G'e^{ig'} & H'e^{ih'} & K'e^{ik'} \end{pmatrix}. \tag{2.1}$$

We look for maximum zero textures (minimum number of parameters) of m_e such that $\det(m_e m_e^\dagger) \neq 0$ (or non-zero eigenvalues for m_e). A careful inspection of the determinant $det(m_e m_e^\dagger)$ reveals six stringent possibilities and are presented accordingly in Table 1. Interestingly, for all these matrices,

Table 1: Minimal textures of the charged lepton mass matrix m_e

$m_e^{(1)} = \begin{pmatrix} A'e^{ia'} & 0 & 0 \\ 0 & B'e^{ib'} & 0 \\ 0 & 0 & C'e^{ic'} \end{pmatrix}$	$m_e^{(2)} = \begin{pmatrix} 0 & 0 & A'e^{ia'} \\ 0 & B'e^{ib'} & 0 \\ C'e^{ic'} & 0 & 0 \end{pmatrix}$	$m_e^{(3)} = \begin{pmatrix} A'e^{ia'} & 0 & 0 \\ 0 & 0 & B'e^{ib'} \\ 0 & C'e^{ic'} & 0 \end{pmatrix}$
$m_e^{(4)} = \begin{pmatrix} 0 & 0 & A'e^{ia'} \\ B'e^{ib'} & 0 & 0 \\ 0 & C'e^{ic'} & 0 \end{pmatrix}$	$m_e^{(5)} = \begin{pmatrix} 0 & A'e^{ia'} & 0 \\ 0 & 0 & B'e^{ib'} \\ C'e^{ic'} & 0 & 0 \end{pmatrix}$	$m_e^{(6)} = \begin{pmatrix} 0 & A'e^{ia'} & 0 \\ B'e^{ib'} & 0 & 0 \\ 0 & 0 & C'e^{ic'} \end{pmatrix}$

$m_e m_e^\dagger$ is diagonal. The matrix (U_l) that diagonalizes $m_e m_e^\dagger$ is an unit matrix and therefore, the mixing arises only from the neutrino sector of the Lagrangian since $U_{PMNS} = U_l{}^\dagger U_\nu$.

3 Texture zeros in Linear seesaw

If A is an invertible $n \times n$ square matrix, and B and C are $n \times m$ matrices, then

$$det(A + BC^T) = det(I_m + C^T A^{-1} B) detA \tag{3.1}$$

Therefore, if we assume $\det(m_\nu) \neq 0$, the Linear Seesaw formula implies that $det(M m^{-1} m_D^T) \neq 0$. Therefore, M, m^{-1} and m_D^T must be non-singular. Since, for a matrix A, $det(A) = det(A^T)$, $det(A^{-1}) = 1/det(A)$, we obtain that m_D, M and m must be non-singular. These leads to the following textures of m_D, M and m and are shown in Table 2, Table 3 and Table 4 respectively.

Table 2: Minimal (6-zero) textures of m_D with $det(m_D) \neq 0$

Minimal (6-zero) textures of m_D with $det(m_D) \neq 0$		
$m_D^{(1)} = \begin{pmatrix} Ae^{ia} & 0 & 0 \\ 0 & Be^{ib} & 0 \\ 0 & 0 & Ce^{ic} \end{pmatrix}$	$m_D^{(2)} = \begin{pmatrix} 0 & 0 & Ae^{ia} \\ 0 & Be^{ib} & 0 \\ Ce^{ic} & 0 & 0 \end{pmatrix}$	$m_D^{(3)} = \begin{pmatrix} Ae^{ia} & 0 & 0 \\ 0 & 0 & Be^{ib} \\ 0 & Ce^{ic} & 0 \end{pmatrix}$
$m_D^{(4)} = \begin{pmatrix} 0 & 0 & Ae^{ia} \\ Be^{ib} & 0 & 0 \\ 0 & Ce^{ic} & 0 \end{pmatrix}$	$m_D^{(5)} = \begin{pmatrix} 0 & Ae^{ia} & 0 \\ 0 & 0 & Be^{ib} \\ Ce^{ic} & 0 & 0 \end{pmatrix}$	$m_D^{(6)} = \begin{pmatrix} 0 & Ae^{ia} & 0 \\ Be^{ib} & 0 & 0 \\ 0 & 0 & Ce^{ic} \end{pmatrix}$

Table 3: Minimal (6-zero) textures of M with $det(M) \neq 0$

Minimal (6-zero) textures of M with $det(M) \neq 0$		
$M^{(1)} = \begin{pmatrix} Xe^{ix} & 0 & 0 \\ 0 & Ye^{iy} & 0 \\ 0 & 0 & Ze^{iz} \end{pmatrix}$	$M^{(2)} = \begin{pmatrix} 0 & 0 & Xe^{ix} \\ 0 & Ye^{iy} & 0 \\ Ze^{iz} & 0 & 0 \end{pmatrix}$	$M^{(3)} = \begin{pmatrix} Xe^{ix} & 0 & 0 \\ 0 & 0 & Ye^{iy} \\ 0 & Ze^{iz} & 0 \end{pmatrix}$
$M^{(4)} = \begin{pmatrix} 0 & 0 & Xe^{ix} \\ Ye^{iy} & 0 & 0 \\ 0 & Ze^{iz} & 0 \end{pmatrix}$	$M^{(5)} = \begin{pmatrix} 0 & Xe^{ix} & 0 \\ 0 & 0 & Ye^{iy} \\ Ze^{iz} & 0 & 0 \end{pmatrix}$	$M^{(6)} = \begin{pmatrix} 0 & Xe^{ix} & 0 \\ Ye^{iy} & 0 & 0 \\ 0 & 0 & Ze^{iz} \end{pmatrix}$

Table 4: Minimal (6-zero) textures of m with $det(m) \neq 0$

Minimal (6-zero) textures of m with $det(m) \neq 0$		
$m^{(1)} = \begin{pmatrix} Pe^{ip} & 0 & 0 \\ 0 & Qe^{iq} & 0 \\ 0 & 0 & Re^{ir} \end{pmatrix}$	$m^{(2)} = \begin{pmatrix} 0 & 0 & Pe^{ip} \\ 0 & Qe^{iq} & 0 \\ Re^{ir} & 0 & 0 \end{pmatrix}$	$m^{(3)} = \begin{pmatrix} Pe^{ip} & 0 & 0 \\ 0 & 0 & Qe^{iq} \\ 0 & Re^{ir} & 0 \end{pmatrix}$
$m^{(4)} = \begin{pmatrix} 0 & 0 & Pe^{ip} \\ Qe^{iq} & 0 & 0 \\ 0 & Re^{ir} & 0 \end{pmatrix}$	$m^{(5)} = \begin{pmatrix} 0 & Pe^{ip} & 0 \\ 0 & 0 & Qe^{iq} \\ Re^{ir} & 0 & 0 \end{pmatrix}$	$m^{(6)} = \begin{pmatrix} 0 & Pe^{ip} & 0 \\ Qe^{iq} & 0 & 0 \\ 0 & 0 & Re^{ir} \end{pmatrix}$

3.1 Effective m_ν in Linear seesaw

Our basic requirement is to admit a structure of m_ν is based on the result of Ref. [22] in which it is shown that to obtain a phenomenologically viable m_ν, the number of independent zeros should be atleast two. Keeping such criterion in view we start with maximum number of zeros in the matrix m for a given m_D and M. It turns out that for 6 zeros in m, all the emerged m_ν has either three or more independent zeros. Discarding such textures, therefore, we start with five zero textures of m. In general, there are 126 possible 5-zero textures of m. But implementation of Linear seesaw, as well as our demand of non-zero eigenvalues of m_ν requires m to be non-singular. The requirement drastically reduces the number of non-singular 5-zero textures of m to 36 which are presented in Table 5.

Table 5: Viable 5-zero textures of m

5 zero textures of m		
$m^1 = \begin{pmatrix} Pe^{ip} & Se^{is} & 0 \\ 0 & Qe^{iq} & 0 \\ 0 & 0 & Re^{ir} \end{pmatrix}$	$m^2 = \begin{pmatrix} Pe^{ip} & 0 & Se^{is} \\ 0 & Qe^{iq} & 0 \\ 0 & 0 & Re^{ir} \end{pmatrix}$	$m^3 = \begin{pmatrix} Pe^{ip} & 0 & 0 \\ Se^{is} & Qe^{iq} & 0 \\ 0 & 0 & Re^{ir} \end{pmatrix}$
$m^4 = \begin{pmatrix} Pe^{ip} & 0 & 0 \\ 0 & Qe^{iq} & Se^{is} \\ 0 & 0 & Re^{ir} \end{pmatrix}$	$m^5 = \begin{pmatrix} Pe^{ip} & 0 & 0 \\ 0 & Qe^{iq} & 0 \\ Se^{is} & 0 & Re^{ir} \end{pmatrix}$	$m^6 = \begin{pmatrix} Pe^{ip} & 0 & 0 \\ 0 & Qe^{iq} & 0 \\ 0 & Se^{is} & Re^{ir} \end{pmatrix}$
$m^7 = \begin{pmatrix} Se^{is} & Pe^{ip} & 0 \\ Qe^{iq} & 0 & 0 \\ 0 & 0 & Re^{ir} \end{pmatrix}$	$m^8 = \begin{pmatrix} 0 & Pe^{ip} & Se^{is} \\ Qe^{iq} & 0 & 0 \\ 0 & 0 & Re^{ir} \end{pmatrix}$	$m^9 = \begin{pmatrix} 0 & Pe^{ip} & 0 \\ Qe^{iq} & Se^{is} & 0 \\ 0 & 0 & Re^{ir} \end{pmatrix}$
$m^{10} = \begin{pmatrix} 0 & Pe^{ip} & 0 \\ Qe^{iq} & 0 & Se^{is} \\ 0 & 0 & Re^{ir} \end{pmatrix}$	$m^{11} = \begin{pmatrix} 0 & Pe^{ip} & 0 \\ Qe^{iq} & 0 & 0 \\ Se^{is} & 0 & Re^{ir} \end{pmatrix}$	$m^{12} = \begin{pmatrix} 0 & Pe^{ip} & 0 \\ Qe^{iq} & 0 & 0 \\ 0 & Se^{is} & Re^{ir} \end{pmatrix}$
$m^{13} = \begin{pmatrix} Se^{is} & 0 & Pe^{ip} \\ Qe^{iq} & 0 & 0 \\ 0 & Re^{ir} & 0 \end{pmatrix}$	$m^{14} = \begin{pmatrix} 0 & Se^{is} & Pe^{ip} \\ Qe^{iq} & 0 & 0 \\ 0 & Re^{ir} & 0 \end{pmatrix}$	$m^{15} = \begin{pmatrix} 0 & 0 & Pe^{ip} \\ Qe^{iq} & Se^{is} & 0 \\ 0 & Re^{ir} & 0 \end{pmatrix}$
$m^{16} = \begin{pmatrix} 0 & 0 & Pe^{ip} \\ Qe^{iq} & 0 & Se^{is} \\ 0 & Re^{ir} & 0 \end{pmatrix}$	$m^{17} = \begin{pmatrix} 0 & 0 & Pe^{ip} \\ Qe^{iq} & 0 & 0 \\ Se^{is} & Re^{ir} & 0 \end{pmatrix}$	$m^{18} = \begin{pmatrix} 0 & 0 & Pe^{ip} \\ Qe^{iq} & 0 & 0 \\ 0 & Re^{ir} & Se^{is} \end{pmatrix}$
$m^{19} = \begin{pmatrix} Se^{is} & Pe^{ip} & 0 \\ 0 & 0 & Qe^{iq} \\ Re^{ir} & 0 & 0 \end{pmatrix}$	$m^{20} = \begin{pmatrix} 0 & Pe^{ip} & Se^{is} \\ 0 & 0 & Qe^{iq} \\ Re^{ir} & 0 & 0 \end{pmatrix}$	$m^{21} = \begin{pmatrix} 0 & Pe^{ip} & 0 \\ Se^{is} & 0 & Qe^{iq} \\ Re^{ir} & 0 & 0 \end{pmatrix}$
$m^{22} = \begin{pmatrix} 0 & Pe^{ip} & 0 \\ 0 & Se^{is} & Qe^{iq} \\ Re^{ir} & 0 & 0 \end{pmatrix}$	$m^{23} = \begin{pmatrix} 0 & Pe^{ip} & 0 \\ 0 & 0 & Qe^{iq} \\ Re^{ir} & Se^{is} & 0 \end{pmatrix}$	$m^{24} = \begin{pmatrix} 0 & Pe^{ip} & 0 \\ 0 & 0 & Qe^{iq} \\ Re^{ir} & 0 & Se^{is} \end{pmatrix}$
$m^{25} = \begin{pmatrix} Pe^{ip} & Se^{is} & 0 \\ 0 & 0 & Qe^{iq} \\ 0 & Re^{ir} & 0 \end{pmatrix}$	$m^{26} = \begin{pmatrix} Pe^{ip} & 0 & Se^{is} \\ 0 & 0 & Qe^{iq} \\ 0 & Re^{ir} & 0 \end{pmatrix}$	$m^{27} = \begin{pmatrix} Pe^{ip} & 0 & 0 \\ Se^{is} & 0 & Qe^{iq} \\ 0 & Re^{ir} & 0 \end{pmatrix}$
$m^{28} = \begin{pmatrix} Pe^{ip} & 0 & 0 \\ 0 & Se^{is} & Qe^{iq} \\ 0 & Re^{ir} & 0 \end{pmatrix}$	$m^{29} = \begin{pmatrix} Pe^{ip} & 0 & 0 \\ 0 & 0 & Qe^{iq} \\ Se^{is} & Re^{ir} & 0 \end{pmatrix}$	$m^{30} = \begin{pmatrix} Pe^{ip} & 0 & 0 \\ 0 & 0 & Qe^{iq} \\ 0 & Re^{ir} & Se^{is} \end{pmatrix}$
$m^{31} = \begin{pmatrix} Se^{is} & 0 & Pe^{ip} \\ 0 & Qe^{iq} & 0 \\ Re^{ir} & 0 & 0 \end{pmatrix}$	$m^{32} = \begin{pmatrix} 0 & Se^{is} & Pe^{ip} \\ 0 & Qe^{iq} & 0 \\ Re^{ir} & 0 & 0 \end{pmatrix}$	$m^{33} = \begin{pmatrix} 0 & 0 & Pe^{ip} \\ Se^{is} & Qe^{iq} & 0 \\ Re^{ir} & 0 & 0 \end{pmatrix}$
$m^{34} = \begin{pmatrix} 0 & 0 & Pe^{ip} \\ 0 & Qe^{iq} & Se^{is} \\ Re^{ir} & 0 & 0 \end{pmatrix}$	$m^{35} = \begin{pmatrix} 0 & 0 & Pe^{ip} \\ 0 & Qe^{iq} & 0 \\ Re^{ir} & Se^{is} & 0 \end{pmatrix}$	$m^{36} = \begin{pmatrix} 0 & 0 & Pe^{ip} \\ 0 & Qe^{iq} & 0 \\ Re^{ir} & 0 & Se^{is} \end{pmatrix}$

Interestingly, only the combinations given in Table (Table 6) gives rise to phenomenologically viable m_ν and all of them leads to a single generic structure as

$$\begin{pmatrix} \times & \times & \times \\ \times & 0 & \times \\ \times & \times & 0 \end{pmatrix}. \tag{3.2}$$

All the other combinations are discarded because they either lead to 3 independent zeros or 2 independent zeros that are not consistent with the current data. For a compact view we present a Table (Table 6) that contains all the allowed combinations of m_D, M and m.

Table 6: Compositions for Allowed Realizations of m_ν

	$M \rightarrow$					
$m_D \downarrow$	$M^{(1)}$	$M^{(2)}$	$M^{(3)}$	$M^{(4)}$	$M^{(5)}$	$M^{(6)}$
$m_D^{(1)}$	m^{16}, m^{23}	m^{12}, m^{17}	m^{9}, m^{36}	m^{5}, m^{22}	m^{3}, m^{18}	m^{29}, m^{34}
$m_D^{(2)}$	m^{10}, m^{25}	m^{14}, m^{21}	m^{2}, m^{15}	m^{28}, m^{31}	m^{8}, m^{33}	m^{4}, m^{19}
$m_D^{(3)}$	m^{9}, m^{36}	m^{5}, m^{22}	m^{16}, m^{23}	m^{12}, m^{27}	m^{29}, m^{34}	m^{3}, m^{18}
$m_D^{(4)}$	m^{2}, m^{15}	m^{28}, m^{31}	m^{10}, m^{25}	m^{14}, m^{21}	m^{4}, m^{19}	m^{8}, m^{33}
$m_D^{(5)}$	m^{1}, m^{24}	m^{11}, m^{32}	m^{26}, m^{35}	m^{6}, m^{13}	m^{17}, m^{20}	m^{7}, m^{30}
$m_D^{(6)}$	m^{26}, m^{35}	m^{6}, m^{13}	m^{1}, m^{24}	m^{11}, m^{31}	m^{7}, m^{30}	m^{17}, m^{20}

Moreover, the transpose and inverse of the above 3 zero textures of m are such that they yield same 3 zero textures. Thus the seesaw formula implies if 5-zero textures are assumed in M (instead in m) and 6 zeros in m and m_D, the resulting textures will be identical to the case where m_D is assumed to have 5-zeros and remaining matrices m, M contain 6 zeros. It turns out that none of the permutations generate two-zero textures other than the one already obtained above.

3.1.1 Parametrization and phase rotation

To be explicit, we parametrize one set of combination (m_D^3 and m^9) and (m_D^3 and m^{36}) which gives rise to m_ν given in Eq.(3.2). To extract the relevant phases out of these allowed m_ν, let us parametrize them in a generic way as

$$m_\nu \;=\; \begin{pmatrix} K_1 e^{ik_1} & K_2 e^{ik_2} & K_3 e^{ik_3} \\ K_2 e^{ik_2} & 0 & K_4 e^{ik_4} \\ K_3 e^{ik_3} & K_4 e^{ik_4} & 0 \end{pmatrix} \tag{3.3}$$

where for m_D^3 with m^9 combination:

$$K_1 e^{ik_1} = \frac{2Ae^{ia-ip-iq+is+ix}SX}{PQ}, \quad K_2 e^{ik_2} = -\frac{Ae^{ia-ip+iy}Y}{P},$$
$$K_3 e^{ik_3} = -\frac{Ce^{ic-iq+ix}X}{Q}, \quad K_4 e^{ik_4} = -\frac{Be^{ib-ir+iz}Z}{R}. \tag{3.4}$$

and for m_D^3 with m^{36} combination:

$$K_1 e^{ik_1} = \frac{2Ae^{ia-ip-ir+is+ix}SX}{PR}, \quad K_2 e^{ik_2} = -\frac{Be^{ib-ir+ix}X}{R},$$
$$K_3 e^{ik_3} = -\frac{Ae^{ia-ip+iz}Z}{P}, \quad K_4 e^{ik_4} = -\frac{Ce^{ic-iq+iy}Y}{Q}. \tag{3.5}$$

4 Texture zeros in Inverse seesaw

As before we consider the minimal non-singular textures of m_D (presented in Table 2) and m (Table 7) whereas the minimal texture of μ_S contains only two-independent complex parameters due to its anti-symmetry and given by the 3 possible textures presented in Table 8.

Table 7: Minimal (6-zero) textures of m

Minimal (6-zero) textures of m		
$m^{(1)} = \begin{pmatrix} Xe^{ix} & 0 & 0 \\ 0 & Ye^{iy} & 0 \\ 0 & 0 & Ze^{iz} \end{pmatrix}$	$m^{(2)} = \begin{pmatrix} 0 & 0 & Xe^{ix} \\ 0 & Ye^{iy} & 0 \\ Ze^{iz} & 0 & 0 \end{pmatrix}$	$m^{(3)} = \begin{pmatrix} Xe^{ix} & 0 & 0 \\ 0 & 0 & Ye^{iy} \\ 0 & Ze^{iz} & 0 \end{pmatrix}$
$m^{(4)} = \begin{pmatrix} 0 & 0 & Xe^{ix} \\ Ye^{iy} & 0 & 0 \\ 0 & Ze^{iz} & 0 \end{pmatrix}$	$m^{(5)} = \begin{pmatrix} 0 & Xe^{ix} & 0 \\ 0 & 0 & Ye^{iy} \\ Ze^{iz} & 0 & 0 \end{pmatrix}$	$m^{(6)} = \begin{pmatrix} 0 & Xe^{ix} & 0 \\ Ye^{iy} & 0 & 0 \\ 0 & 0 & Ze^{iz} \end{pmatrix}$

Table 8: Minimal (4-independent zero) textures of μ_S

Minimal (4-independent zero) textures of μ_S		
$\mu_S^{(1)} = \begin{pmatrix} 0 & 0 & Re^{ir} \\ 0 & Se^{is} & 0 \\ Re^{ir} & 0 & 0 \end{pmatrix}$	$\mu_S^{(2)} = \begin{pmatrix} Pe^{ip} & 0 & 0 \\ 0 & 0 & Te^{it} \\ 0 & Te^{it} & 0 \end{pmatrix}$	$\mu_S^{(3)} = \begin{pmatrix} 0 & Qe^{iq} & 0 \\ Qe^{iq} & 0 & 0 \\ 0 & 0 & Ve^{iv} \end{pmatrix}$

However, it turns out that if the number of zeros in μ_S is greater than 3 (as in Table 8), all the emerged m_ν contain 3 or more independent zeros and hence discarded. Therefore, to obtain

viable structures of m_ν we stick with the non-singular 2 zero textures of μ_S and are presented in Table 9. Interestingly, unlike Linear seesaw, we note that Inverse seesaw leads to all the 7 viable two-zero textures (m_ν^1 - m_ν^7) of m_ν given in Ref. [22]. In a compact way, in Table 10 we present all the combinations that generate these textures of m_ν.

Table 9: 2-independent zero textures for μ_S

2-independent-zero textures for μ_S		
$\mu_S^1 = \begin{pmatrix} 0 & 0 & Re^{ir} \\ 0 & Se^{is} & Te^{it} \\ Re^{ir} & Te^{it} & Ve^{iv} \end{pmatrix}$	$\mu_S^2 = \begin{pmatrix} 0 & Qe^{iq} & Re^{ir} \\ Qe^{iq} & Se^{is} & 0 \\ Re^{ir} & 0 & Ve^{iv} \end{pmatrix}$	$\mu_S^3 = \begin{pmatrix} 0 & Qe^{iq} & 0 \\ Qe^{iq} & Se^{is} & Te^{it} \\ 0 & Te^{it} & Ve^{iv} \end{pmatrix}$
$\mu_S^4 = \begin{pmatrix} Pe^{ip} & 0 & Re^{ir} \\ 0 & 0 & Te^{it} \\ Re^{ir} & Te^{it} & Ve^{iv} \end{pmatrix}$	$\mu_S^5 = \begin{pmatrix} Pe^{ip} & Qe^{iq} & Re^{ir} \\ Qe^{iq} & 0 & 0 \\ Re^{ir} & 0 & Ve^{iv} \end{pmatrix}$	$\mu_S^6 = \begin{pmatrix} Pe^{ip} & Qe^{iq} & 0 \\ Qe^{iq} & 0 & Te^{it} \\ 0 & Te^{it} & Ve^{iv} \end{pmatrix}$
$\mu_S^7 = \begin{pmatrix} Pe^{ip} & 0 & Re^{ir} \\ 0 & Se^{is} & Te^{it} \\ Re^{ir} & Te^{it} & 0 \end{pmatrix}$	$\mu_S^8 = \begin{pmatrix} Pe^{ip} & Qe^{iq} & Re^{ir} \\ Qe^{iq} & Se^{is} & 0 \\ Re^{ir} & 0 & 0 \end{pmatrix}$	$\mu_S^9 = \begin{pmatrix} Pe^{ip} & Qe^{iq} & 0 \\ Qe^{iq} & Se^{is} & Te^{it} \\ 0 & Te^{it} & 0 \end{pmatrix}$
$\mu_S^{10} = \begin{pmatrix} Pe^{ip} & Qe^{iq} & Re^{ir} \\ Qe^{iq} & 0 & Te^{it} \\ Re^{ir} & Te^{it} & 0 \end{pmatrix}$	$\mu_S^{11} = \begin{pmatrix} 0 & Qe^{iq} & Re^{ir} \\ Qe^{iq} & Se^{is} & Te^{it} \\ Re^{ir} & Te^{it} & 0 \end{pmatrix}$	$\mu_S^{12} = \begin{pmatrix} 0 & Qe^{iq} & Re^{ir} \\ Qe^{iq} & 0 & Te^{it} \\ Re^{ir} & Te^{it} & Ve^{iv} \end{pmatrix}$

Table 10: Compositions for Realization of two-zero m_ν textures with $m_D = m_D^{(1)}$

	$m \rightarrow$					
μ_S $\downarrow$	m^1	m^2	m^3	m^4	m^5	m^6
μ_S^1	m_ν^1	$\times$	m_ν^2	m_ν^6	$\times$	m_ν^5
μ_S^2	$\times$	m_ν^4	$\times$	m_ν^4	m_ν^3	m_ν^3
μ_S^3	m_ν^2	m_ν^6	m_ν^1	$\times$	$\times$	$\times$
μ_S^4	m_ν^5	$\times$	m_ν^6	m_ν^2	m_ν^5	m_ν^1
μ_S^5	$\times$	m_ν^5	$\times$	m_ν^1	$\times$	m_ν^2
μ_S^6	m_ν^3	m_ν^3	m_ν^4	$\times$	m_ν^6	$\times$
μ_S^7	m_ν^4	$\times$	m_ν^3	m_ν^3	m_ν^4	m_ν^4
μ_S^8	$\times$	m_ν^1	$\times$	m_ν^5	m_ν^2	m_ν^6
μ_S^9	m_ν^6	m_ν^2	m_ν^5	$\times$	m_ν^1	$\times$
μ_S^{10}	m_ν^7	$\times$	m_ν^7	$\times$	$\times$	$\times$
μ_S^{11}	$\times$	$\times$	$\times$	m_ν^7	$\times$	m_ν^7
μ_S^{12}	$\times$	m_ν^7	$\times$	$\times$	m_ν^7	$\times$

Similar to Table 10, five more tables can be obtained for $m_D^{(2)} - m_D^{(6)}$. However, all those combinations also lead to all seven possible two-zero textures but with different combinations of m_D, m and μ_S. We are not listing all these tables.

4.1 Effective m_ν and its parametrization

We parametrize all emerged viable m_ν matrices in Table 11 in a generic way where K_i and k_i are functions of the elements of m_D, m and μ_S. We are not listing explicit expressions of each K_i and k_i parameters as there are many different functions for K_i and k_i.

4.2 Numerical analysis

The matrix m_ν obtained in Linear seesaw case Eqn.(3.5) is similar to the matrix m_ν^7 obtained in Inverse seesaw case. In order to perform the numerical analysis we use the experimental constraints (Table 12) arising from the global fit oscillation data. We note that the first two matrices (m_ν^1 and m_ν^2) of Table 11 do not trigger $\beta\beta_{0\nu}$ decay, due to $|m_{11}| = 0$ for these two matrices. Therefore, we categorize all the matrices presented in Table 11 into two different classes.

Class I: Parameter ranges for allowed m_ν with $|m_{11}| \neq 0$

Table 11: Effective allowed m_ν from Inverse seesaw

Effective allowed m_ν from Inverse seesaw		
m_ν	Phase rotated m_ν	Parametrization
$m_\nu^1 = \begin{pmatrix} 0 & 0 & K_1 e^{ik_1} \\ 0 & K_2 e^{ik_2} & K_3 e^{ik_3} \\ K_1 e^{ik_1} & K_3 e^{ik_3} & K_4 e^{ik_4} \end{pmatrix}$	$m_\nu^1 = m_0 \begin{pmatrix} 0 & 0 & 1 \\ 0 & y_1 & y_2 \\ 0 & y_2 & y_3 e^{i\alpha} \end{pmatrix}$	$m_0 = K_1,\ K_2/K_1 = y_1,$ $K_3/K_1 = y_2,\ K_4/K_1 = y_3,$ $\alpha = (k_2 - 2k_3 + k_4)$
$m_\nu^2 = \begin{pmatrix} 0 & K_1 e^{ik_1} & 0 \\ K_1 e^{ik_1} & K_2 e^{ik_2} & K_3 e^{ik_3} \\ 0 & K_3 e^{ik_3} & K_4 e^{ik_4} \end{pmatrix}$	$m_\nu^2 = m_0 \begin{pmatrix} 0 & 1 & 0 \\ 1 & y_1 & y_2 \\ 0 & y_2 & y_3 e^{i\alpha} \end{pmatrix}$	$m_0 = K_1,\ K_2/K_1 = y_1,$ $K_3/K_1 = y_2,\ K_4/K_1 = y_3,$ $\alpha = (k_2 - 2k_3 + k_4)$
$m_\nu^3 = \begin{pmatrix} K_1 e^{ik_1} & K_2 e^{ik_2} & 0 \\ K_2 e^{ik_2} & 0 & K_3 e^{ik_3} \\ 0 & K_3 e^{ik_3} & K_4 e^{ik_4} \end{pmatrix}$	$m_\nu^3 = m_0 \begin{pmatrix} 1 & y_1 & 0 \\ y_1 & 0 & y_2 \\ 0 & y_2 & y_3 e^{i\alpha} \end{pmatrix}$	$m_0 = K_1,\ K_2/K_1 = y_1,$ $K_3/K_1 = y_2,\ K_4/K_1 = y_3,$ $\alpha = (2k_2 - 2k_3 + k_4 - k_1)$
$m_\nu^4 = \begin{pmatrix} K_1 e^{ik_1} & 0 & K_2 e^{ik_2} \\ 0 & K_4 e^{ik_4} & K_3 e^{ik_3} \\ K_2 e^{ik_2} & K_3 e^{ik_3} & 0 \end{pmatrix}$	$m_\nu^4 = m_0 \begin{pmatrix} 1 & 0 & y_1 \\ 0 & y_3 & y_2 e^{i\alpha} \\ y_1 & y_2 e^{i\alpha} & 0 \end{pmatrix}$	$m_0 = K_1,\ K_2/K_1 = y_1,$ $K_3/K_1 = y_2,\ K_4/K_1 = y_3,$ $\alpha = \frac{1}{2}(k_1 - 2k_2 + 2k_3 - k_4)$
$m_\nu^5 = \begin{pmatrix} K_1 e^{ik_1} & 0 & K_2 e^{ik_2} \\ 0 & 0 & K_3 e^{ik_3} \\ K_2 e^{ik_2} & K_3 e^{ik_3} & K_4 e^{ik_4} \end{pmatrix}$	$m_\nu^5 = m_0 \begin{pmatrix} 0 & 0 & y_1 \\ 0 & 0 & y_2 \\ y_1 & y_2 & y_3 e^{i\alpha} \end{pmatrix}$	$m_0 = K_1,\ K_2/K_1 = y_1,$ $K_3/K_1 = y_2,\ K_4/K_1 = y_3,$ $\alpha = (k_1 - 2k_2 + k_4)$
$m_\nu^6 = \begin{pmatrix} K_1 e^{ik_1} & K_2 e^{ik_2} & 0 \\ K_2 e^{ik_2} & K_4 e^{ik_4} & K_3 e^{ik_3} \\ 0 & K_3 e^{ik_3} & 0 \end{pmatrix}$	$m_\nu^6 = m_0 \begin{pmatrix} 1 & y_1 & 0 \\ y_1 & y_3 e^{i\alpha} & y_2 \\ 0 & y_2 & 0 \end{pmatrix}$	$m_0 = K_1,\ K_2/K_1 = y_1,$ $K_3/K_1 = y_2,\ K_4/K_1 = y_3,$ $\alpha = (k_1 - 2k_2 + k_4)$
$m_\nu^7 = \begin{pmatrix} K_1 e^{ik_1} & K_2 e^{ik_2} & K_3 e^{ik_3} \\ K_2 e^{ik_2} & 0 & K_4 e^{ik_4} \\ K_3 e^{ik_3} & K_4 e^{ik_4} & 0 \end{pmatrix}$	$m_\nu^7 = m_0 \begin{pmatrix} y_1 & 1 & y_2 \\ 1 & 0 & y_3 e^{i\alpha} \\ y_2 & y_3 e^{i\alpha} & 0 \end{pmatrix}$	$m_0 = K_2,\ K_1/K_2 = y_1,$ $K_3/K_2 = y_2,\ K_4/K_2 = y_3,$ $\alpha = (k_1 - k_2 - k_3 + k_4).$

For the numerical analysis of the matrices $m_\nu^3, m_\nu^4, m_\nu^5, m_\nu^6$ we use the experimental constraints (Table 12) arising from the global fit oscillation data. It is seen that all the parameters are constrained in a very narrow range and we present them in Table 13. The matrices predict a constrained

Table 12: Input experimental values [42]

Quantity	3σ ranges
$\lvert\Delta m^2_{31}\rvert$ (N)	$2.30 < \Delta m^2_{31}(10^3 eV^{-2}) < 2.64$
$\lvert\Delta m^2_{31}\rvert$ (I)	$2.20 < \Delta m^2_{31}(10^3 eV^{-2}) < 2.54$
Δm^2_{21}	$7.11 < \Delta m^2_{21}(10^5 eV^{-2}) < 8.18$
θ_{12}	$31.8^o < \theta_{12} < 37.8^o$
θ_{23}	$39.4^o < \theta_{23} < 53.1^o$
θ_{13}	$8^o < \theta_{13} < 9.4^o$

range of δ_{CP} phase along with an upper bound on the sum of three light neutrino masses ($\Sigma_i m_i$) well below the upper limit dictated by the PLANCK and other astrophysical experiments [43]. For all the four matrices we get normal hierarchical spectrum of neutrino masses. The value of m_{11} are also far below the present experimental probing region [44] .

Table 13: Parameter ranges of the matrices with $|m_{11}| \neq 0$

m_ν	y_1, y_2, y_3	$\lvert\delta_{CP}\rvert$ (deg)	$J_{CP} \times 10^3$	$\sum m_i$ (eV)	$\lvert m_{11}\rvert$ (eV)$\times 10^2$
m^3_ν	$y_1 : 0.06 - 0.125$, $y_2 : 1.11 - 1.23$, $y_3 : 0.24 - 0.50$	$3.96 - 5.25$	$2.3 - 3.6$	$0.146 - 0.215$	$4.2 - 6.8$
m^4_ν	$y_1 : 0.06 - 0.23$, $y_2 : 1.118 - 1.386$, $y_3 : 0.259 - 0.866$	$6.51 - 7.65$	$3.8 - 4.8$	$0.116 - 0.210$	$3 - 6.4$
m^5_ν	$y_1 : (7.98 - 8) \times 10^{-2}$, $y_2 : 1.15 - 1.18$, $y_3 : 0.39 - 0.41$	$9.0 - 9.4$	$5.25 - 5.27$	$0.14 - 0.172$	$4.8 - 5.1$
m^6_ν	$y_1 : 0.11 - 0.14$, $y_2 : 1.17 - 1.27$, $y_3 : 0.40 - 0.66$	$5.72 - 7.53$	$1.29 - 2.59$	$0.128 - 0.173$	$3.5 - 5.1$
m^7_ν	$y_1 : 1.30 - 1.34$, $y_2 : 0.85 - 0.89$, $y_3 : 0.79 - 0.82$	0	0	$0.127 - 0.131$	$0.022 - 0.023$

Class II: Parameter ranges of the matrices with $|m_{11}| = 0$

Unlike the previous case, this class of matrices (m_ν^1 and m_ν^2) allow a sizable parameter space compatible with the experimental data. However, the matrices also predict constraint ranges of δ_{CP} phase and $\Sigma_i m_i$. We present plots of these parameters in figure 1 and figure 2 respectively. From the first two plots of figure 1 the ranges of the parameters read as $1.69 < y_1 < 2.93$, $1.47 < y_2 < 2.97$ and $1.37 < y_3 < 3.16$.

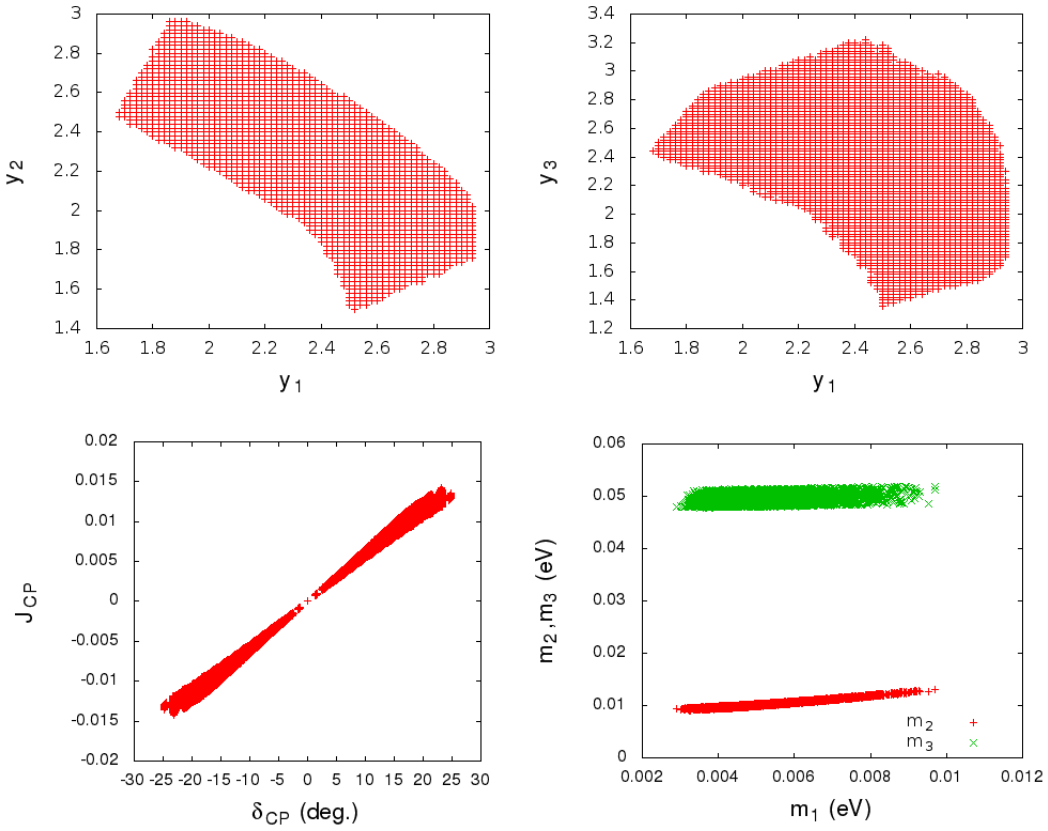

Figure 1: The first two figures of the top row represent the parameter space for m_ν^1 matrix. Left plot of the bottom row is the variation of J_{CP} with δ_{CP} and the right figure shows the hierarchy (normal) of the model.

The Dirac CP phase is constrained as $-25^o < \delta_{CP} < 25^o$ and the sum of the light neutrino masses ($\Sigma_i m_i$) is obtained within the range 0.094 eV $< \Sigma_i m_i <$ 0.18 eV which is well below the present experimental upper bound. In figure 2 we present the parameter ranges for m_ν^2. The matrix m_ν^2 also allow a sizable parameter space and are depicted in first two plots of figure 2. The ranges of y_1, y_2 and y_3 can be read as $1.58 < y_1 < 3.4$, $1.5 < y_2 < 3$ and $1.5 < y_3 < 2.96$. Similar to the previous case, for this matrix also the ranges for δ_{CP} and $\Sigma_i m_i$ are constrained in a very narrow

range as $-8^o < \delta_{CP} < 8^o$, 0.09 eV $< \Sigma_i m_i <$ 0.16 eV. The hierarchy is normal and is depicted in the extreme right plot of the bottom row of figure 2.

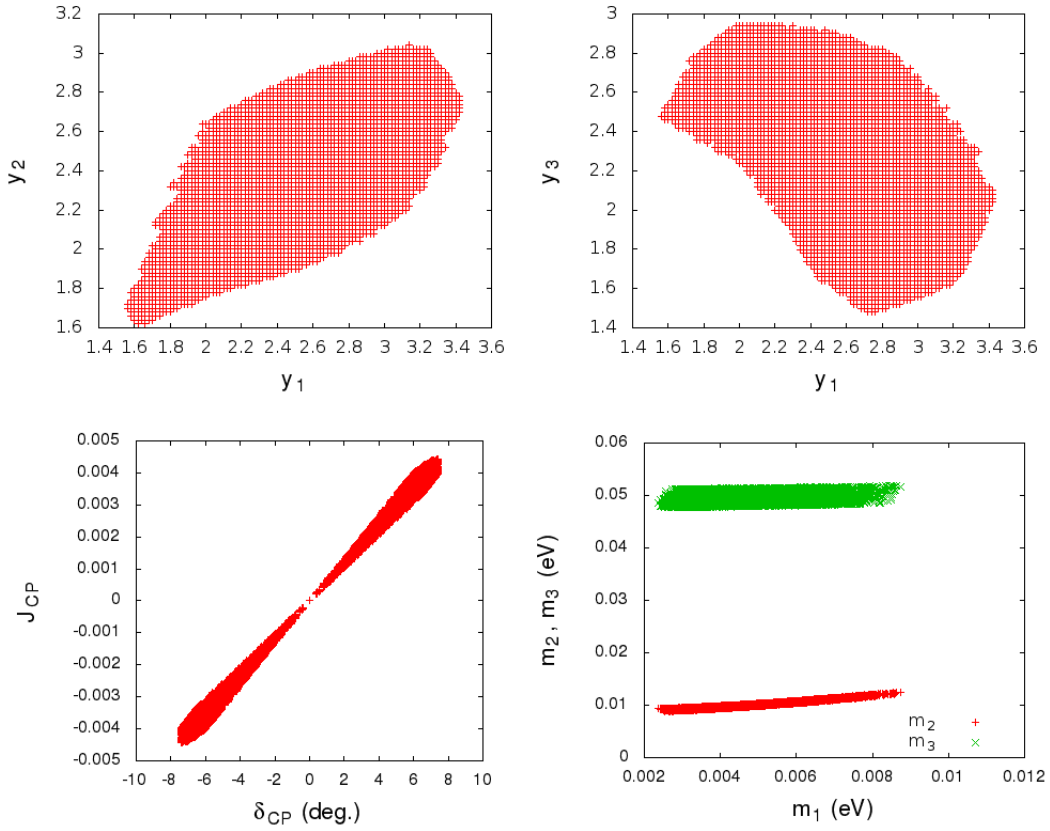

Figure 2: The first two figures of the top row represent the parameter space for m_ν^2 matrix. Left plot of the bottom row is the variation of J_{CP} with δ_{CP} and the right figure shows the hierarchy (normal) of the model.

5 Summary

We analyze two low energy seesaw (Linear seesaw and Inverse seesaw) mechanisms with the assumption of a minimal non-singular structure of the charged lepton mass matrix m_e with three distinct eigenvalues and non-zero eigenvalues for the effective neutrino mass matrix. Non-singular nature of m_e and m_ν dictates certain possible textures for the constituent matrices. In the Linear seesaw, in our minimalistic approach,it is seen that 5 is the maximal number of zeros that can be accommodated in matrix 'm' to obtain phenomenologically viable m_ν. On the other hand, in the inverse seesaw, all the allowed two-zero textures can be explicitly realized in terms of the minimally

parametrized constituent matrices. We have numerically explored the allowed parameter ranges using neutrino oscillation global fit data and predict $\sum m_i$, $|m_{11}|$, J_{CP} and δ_{CP} along with the hierarchical structure of neutrino masses. One of the important prediction of this scheme is the vanishingly small value of δ_{CP} which could be tested by the ongoing T2K experiment. All the matrices predict nonvanishing and highly constrained range of δ_{CP} along with the normal hierarchical spectrum of neutrino masses. Numerical analyses shows that two-zero textures cannot give rise to large CP violation, and therefore if $\delta_{CP} = \pi/2$ is established, this minimal scheme will be ruled out. However, we can possibly continue to have the same scheme in the neutrino sector but with other nontrivial charged lepton mass matrices such that $h_e = m_e m_e^\dagger$ is not diagonal to obtain large CP-violating phase.

References

[1] S. Davidson and A. Ibarra, Phys. Lett. B **535**, 25 (2002) [hep-ph/0202239].

[2] S. Blanchet, P. S. B. Dev and R. N. Mohapatra, Phys. Rev. D **82**, 115025 (2010) [arXiv:1010.1471 [hep-ph]].

[3] J. D. Clarke, R. Foot and R. R. Volkas, Phys. Rev. D **91**, no. 7, 073009 (2015) [arXiv:1502.01352 [hep-ph]].

[4] R. N. Mohapatra and J. W. F. Valle, Phys. Rev. D **34**, 1642 (1986).

[5] J. Bernabeu, A. Santamaria, J. Vidal, A. Mendez and J. W. F. Valle, Phys. Lett. B **187**, 303 (1987).

[6] R. N. Mohapatra, Phys. Rev. Lett. **56**, 561 (1986).

[7] J. Schechter and J. W. F. Valle, Phys. Rev. D **25**, 774 (1982).

[8] J. Schechter and J. W. F. Valle, Phys. Rev. D **22**, 2227 (1980).

[9] S. Fraser, E. Ma and O. Popov, Phys. Lett. B **737**, 280 (2014) [arXiv:1408.4785 [hep-ph]].

[10] A. Ghosal and R. Samanta, JHEP **1505**, 077 (2015) [arXiv:1501.00916 [hep-ph]].

[11] B. Adhikary, A. Ghosal and P. Roy, Indian J. Phys. **88**, 979 (2014) [arXiv:1311.6746 [hep-ph]].

[12] S. S. C. Law and K. L. McDonald, Phys. Rev. D **87**, no. 11, 113003 (2013) [arXiv:1303.4887 [hep-ph]].

[13] P. S. B. Dev and R. N. Mohapatra, Phys. Rev. D **81**, 013001 (2010) [arXiv:0910.3924 [hep-ph]].

[14] A. E. Crcamo Hernndez and R. Martinez, arXiv:1501.05937 [hep-ph].

[15] A. E. Crcamo Hernndez, R. Martnez and F. Ochoa, arXiv:1309.6567 [hep-ph].

[16] A. E. C. Hernndez and I. d. M. Varzielas, J. Phys. G **42**, no. 6, 065002 (2015) doi:10.1088/0954-3899/42/6/065002 [arXiv:1410.2481 [hep-ph]].

[17] S. M. Barr, Phys. Rev. Lett. **92**, 101601 (2004) [hep-ph/0309152].

[18] H. Hettmansperger, M. Lindner and W. Rodejohann, JHEP **1104**, 123 (2011) [arXiv:1102.3432 [hep-ph]].

[19] M. Hirsch, S. Morisi and J. W. F. Valle, Phys. Lett. B **679**, 454 (2009) [arXiv:0905.3056 [hep-ph]].

[20] M. Chakraborty, H. Z. Devi and A. Ghosal, Phys. Lett. B **741**, 210 (2015) [arXiv:1410.3276 [hep-ph]].

[21] W. Wang and Z. L. Han, arXiv:1508.00706 [hep-ph].

[22] P. H. Frampton, S. L. Glashow and D. Marfatia, Phys. Lett. B **536**, 79 (2002) [hep-ph/0201008].

[23] K. Whisnant, J. Liao and D. Marfatia, AIP Conf. Proc. **1604**, 273 (2014).

[24] P. O. Ludl and W. Grimus, JHEP **1407**, 090 (2014) [arXiv:1406.3546 [hep-ph]].

[25] W. Grimus and P. O. Ludl, PoS EPS **-HEP2013**, 075 (2013) [arXiv:1309.7883 [hep-ph]].

[26] J. Liao, D. Marfatia and K. Whisnant, JHEP **1409**, 013 (2014) [arXiv:1311.2639 [hep-ph]].

[27] H. Fritzsch, Z. z. Xing and S. Zhou, JHEP **1109**, 083 (2011) [arXiv:1108.4534 [hep-ph]].

[28] A. Merle and W. Rodejohann, Phys. Rev. D **73**, 073012 (2006) [hep-ph/0603111].

[29] W. Wang, Phys. Lett. B **733**, 320 (2014) [Erratum-ibid. B **738**, 524 (2014)] [arXiv:1401.3949 [hep-ph]].

[30] L. Lavoura, Phys. Lett. B **609**, 317 (2005) [hep-ph/0411232].

[31] A. Kageyama, S. Kaneko, N. Shimoyama and M. Tanimoto, Phys. Lett. B **538**, 96 (2002) [hep-ph/0204291].

[32] W. Wang, Phys. Rev. D **90**, 033014 (2014) [arXiv:1402.6808 [hep-ph]].

[33] S. Baek, H. Okada and K. Yagyu, JHEP **1504**, 049 (2015) [arXiv:1501.01530 [hep-ph]].

[34] G. C. Branco, D. Emmanuel-Costa, M. N. Rebelo and P. Roy, Phys. Rev. D **77** (2008) 053011 [arXiv:0712.0774 [hep-ph]].

[35] S. Choubey, W. Rodejohann and P. Roy, Nucl. Phys. B **808**, 272 (2009) [Erratum-ibid. **818**, 136 (2009)] [arXiv:0807.4289 [hep-ph]].

[36] B. Adhikary, A. Ghosal and P. Roy, JHEP **0910** (2009) 040 [arXiv:0908.2686 [hep-ph]].

[37] B. Adhikary, A. Ghosal and P. Roy, JCAP **1101** (2011) 025 [arXiv:1009.2635 [hep-ph]].

[38] B. Adhikary, A. Ghosal and P. Roy, Mod. Phys. Lett. A **26** (2011) 2427 [arXiv:1103.0665 [hep-ph]].

[39] R. Samanta, M. Chakraborty and A. Ghosal, arXiv:1502.06508 [hep-ph].

[40] R. Samanta and A. Ghosal, arXiv:1507.02582 [hep-ph].

[41] B. Adhikary, M. Chakraborty and A. Ghosal, Phys. Rev. D **86**, 013015 (2012) [arXiv:1205.1355 [hep-ph]].

[42] D. V. Forero, M. Tortola and J. W. F. Valle, Phys. Rev. D **90**, no. 9, 093006 (2014) [arXiv:1405.7540 [hep-ph]].

[43] P. A. R. Ade *et al.* [Planck Collaboration], arXiv:1502.01589 [astro-ph.CO].

[44] M. Auger *et al.* [EXO-200 Collaboration], Phys. Rev. Lett. **109**, 032505 (2012) doi:10.1103/PhysRevLett.109.032505 [arXiv:1205.5608 [hep-ex]].